Behaviour of Lognormally-Distributed Differential Functions of Rain Drop Profiles over Radio Links

Akintunde Alonge, *Member*, *IEEE*
Department of Electrical and Electronic Engineering Technology
University of Johannesburg
Johannesburg, South Africa
aalonge@uj.ac.za

***Abstract*—Rainfall attenuation is undoubtedly one of the factors to be considered in the deployment of outdoor 5G services as the system rollout becomes inevitable. In this paper, the rainfall subject is approached from the microstructure of rain drop sizes, by utilizing derivatives of the Type II Lognormal Drop Size Distribution (DSD) model. DSD measurements from three African locations - Durban, South Africa (29°52′S, 30°58′E), Butare, Rwanda (2°36′S, 29°44′E) and Ile-Ife, Nigeria (7°31′N, 4°31′E) – are investigated as first order and second order Differential Equations (DEs). General expressions representing these DEs are developed and applied to derivative scenarios for different rainfall rate categories: 20 mm/h, 60 mm/h and 110 mm/h. These scenarios represent shower events, thunderstorm events and severe thunderstorm events. Results obtained show that a good overview of DSD variations is realized from these derivatives, when compared with the measured diameter spectrum. The compared DSD characteristics at these selected locations offer an interesting perspective on the behaviour of lognormal distributions at these selected locations.**

***Keywords*—Radio propagation, rain drop size distribution, rainfall attenuation, lognormal distribution, differential equations.**

I. INTRODUCTION

The future of wireless communication is increasingly getting exciting (and truly complex) with systems such as Fifth Generation (5G) cellular communication and Internet of Things (IoT) becoming the new face of telecommunication [1]. As with all futuristic wireless communication systems, these proposed systems are accompanied by serious constraints since new applications and services are offered by service providers. In [2], [3], these constraints affecting wireless systems could be described as an "iron triangle" scenario in which a tripartite combination of data rate, power and range all play huge roles. In fact, these three factors are all related to the propagation limitations often faced by wireless systems. However, what further complicates the envisaged system - is the huge dependency of 5G communication backhaul on frequencies ranging from about 2 GHz up to 100 GHz – all within the microwave and millimeter wave bands [4]. Frequencies within these bands have been proposed as suitable platforms for offering indoor and outdoor services in 5G systems [5].

In [4],[6]-[8], a few theoretical analysis, experimental measurements and white papers have demonstrated that transmitting and receiving at these frequencies for outdoor purposes is possible, albeit with limitations. Because these outdoor wireless systems could be assumed as Line-Of-Sight (LOS) or Non Line-Of-Sight (NLOS), outdoor attenuation will offer a veritable source of concern. In this paper, the effect of rainfall is investigated as one of the outdoor sources of attenuation. Rainfall, being one of the atmospheric hydrometeors responsible for significant signal losses and outages in wireless systems, affects both terrestrial and satellite communication systems [9]. Because rainfall is a local phenomenon, it usually varies in time and space at different locations around the world. Modelling of rainfall parameters have always been approached using its component microstructures such as rainfall rate, rainfall DSD, radar reflectivity and so on. Of these parameters, the International Telecommunication Union (ITU) recommends the most readily available microstructure for radio planning and propagation studies, which is rainfall rate [10]. However, rainfall rate measurement often fails to give a vivid description of the spatial and temporal nature of rainfall events over its location. Therefore, measurements in form of rainfall drop sizes or even radar ensembles are often preferred. In this paper, however, the focus will be on the description of rainfall drop size (or DSD) measurements across different locations.

Measurements of rain drop profiles often give good representation of the scattering and absorption of propagated waves as they pass through any rain medium. The droplet particle size, complex refractive index of water, rainfall rate and signal frequency are important parameters which determine the intensity of scattering and absorption occurring in rainy medium. While the particle size of rain droplets determines how much signal it 'mops up' (absorb) or 'bounces off' (scatter), the frequency of transmission gradually changes the complex refractivity of the water content within the particle size [9], [11]. Most importantly, the probability distribution (or DSD) of rain droplets within the atmosphere during rain events plays a huge role in the determining the instantaneous rainfall attenuation level. Thus, the study of rainfall in radio engineering is useful in the estimation of rainfall attenuation and rain cell statistics. Information on DSDs also provides spatio-temporal understanding of the dynamics of rain attenuation over radio links. Measurement of rain drop profiles is often undertaken by instruments called disdrometer. Because this instrument is expensive to acquire and install, there are few of such measurements from different locations across the world.

In this paper, an investigation is carried out based on results obtained from DSD results from three locations within Africa. The procedure applied here is to understand the variation of DSDs with respect to the particle size (or diameter), hence, the need to employ differential functions. Therefore, the motivation of this paper is to mainly observe the trend of DSD derivatives over the selected locations in Africa. This will enable the concise observation of statistical DSDs relative to changes within the diameter spectrum, in order to determine the level of similarity in such differential profile across locations. The locations considered are Durban, South Africa (29°52′S, 30°58′E), Butare, Rwanda (2°36′S, 29°44′E) and Ile-Ife, Nigeria (7°31′N, 4°31′E). These locations represent diverse climates in subtropical, equatorial and tropical Africa respectively. The rest of this paper shall be as follows: Section

II will cover aspects of lognormally-distributed functions, Section III will discuss measurements and modelling, Section IV will cover results and discussions and finally, Section V concludes the paper.

II. Overview of Lognormally-Distributed Rain Drop Size Functions and Differential Equations

Statistical distributions approximating rain drop size have often been approached by using known probability laws. Because the typical DSD is a scaled version of its fundamental Probability Density Function (PDF), it often modelled using popular statistical models. A plotted DSD against its array of diameters usually appears as an inverted U-shape, with a single peak implying maximum density. Thus, we find from literature certain statistical models which satisfies DSD behaviour to include: Weibull model, lognormal model, modified gamma model and negative exponential model [12]. More importantly, the modified gamma and lognormal models are useful for modelling DSDs in tropical (and subtropical) climates, while the negative exponential model is appropriate for temperate climates. Since climatic locations of the measurements discussed in section II are mainly tropical, subtropical and equatorial - and the lognormal model being a more popular choice - this model is thus considered.

For the purpose of simplicity, lognormal distributions applied in radio engineering (and hydrology) are basically categorized under two distinct categories: Type I lognormal and Type II lognormal distributions. These two lognormal distributions are not typically different from one another in structure, except for minor alterations in the input parameter functions. Mathematically, the Type I lognormal distribution applied in rainfall DSD studies is given by [13]:

$$N(D) = \frac{N_T}{\sqrt{2\pi}D\sigma} e^{\left[-\frac{1}{2}\left(\frac{ln(D)-\mu}{\sigma}\right)^2\right]} \quad \text{for } D \in (0,\infty) \quad (1)$$

In this definition, N_T is described as the rain drop concentration per unit volume, whereas μ and σ represent the mean and standard deviation of the spherical rain drop-sizes respectively.

In the same guise, the Type II lognormal distribution assumes that $\mu = ln(D_g)$ and $\sigma = ln(\sigma_g)$ in (1). Thus, this function becomes [14]:

$$N(D) = \frac{N_T}{\sqrt{2\pi}ln(\sigma_g)D} e^{\left[-\frac{1}{2}\left(\frac{ln^2\left(\frac{D}{D_g}\right)}{ln^2(\sigma_g)}\right)\right]} \quad \text{for } D \in (0,\infty) \quad (2)$$

While the previous definitions in (1) remain valid, D_g and σ_g will assume new definitions called the mean geometric diameter and standard geometric deviation of spherical rain drop-sizes respectively [14].

It should be noted that in this study, the lognormal Type II is the preferred choice for modelling. For this reason, lognormal distribution results modelled as Type I at different measurement sites have been normalized as Type II in this work. Since, it is important to investigate the overall local context of the earlier of rainfall DSD measurements undertaken at Durban [15], Butare [15] and Ile-Ife [16], a procedure is employed to transform (2) into homogeneous DEs. In this procedure, the first and second derivative functions of (2) are sought using the product-rule differentiation principle. In the first step, a first order DE is obtained and a second order DE is obtained in the second step. The procedure applied for the derivation of each DEs is presented in the subsections that follow.

A. First Order Differential Equation: Lognormal Type II

The first derivative of a DSD primarily provides information about its nature and structure, with regards to the instantaneous rate of change with respect to the diameter intervals, which is the function slope. It also provides information about the spread of the DSD along its independent variable, *D*. Mathematically, the initial rate of change of $N(D)$ given by $\frac{d\,N(D)}{dD}$ can be realized as a homogeneous first order differential equation:

$$\frac{d\,\{N(D)\}}{dD} = N'(D) = \alpha N(D) \quad (3)$$

whereas the constant, α, is given as,

$$\alpha = -\left[\frac{ln^2(\sigma_g) + ln\left(\frac{D}{D_g}\right)}{Dln^2(\sigma_g)}\right] \quad (3a)$$

All input parameters retain their existing definitions as given in (2). The expression in (3) gives an overall expression of the rate variation of $N(D)$ over the entire diametric spectrum of the measuring instrument.

B. Second Order Differential Equation: Lognormal Type II

The second derivative of this DSD is simply the derivative of the first order DE in (3). The second derivative may not really give us new information about $N(D)$ but it definitely gives us more information about the spread of the function along its independent variable. Mathematically, the second derivative given by $\frac{d^2N(D)}{dD^2}$ can also be approximated as a homogeneous second order differential equation:

$$\frac{d^2\{N(D)\}}{dD^2} = N''(D) = \beta N'(D) + \gamma N(D) \quad (4)$$

whereas the constants, β and γ, are given as,

$$\beta = -\frac{ln^2(\sigma_g) + ln\left(\frac{D}{D_g}\right)}{Dln^2(\sigma_g)} \quad (4a)$$

And,

$$\gamma = -\frac{1 - ln^2(\sigma_g) - ln\left(\frac{D}{D_g}\right)}{D^2ln^2(\sigma_g)} \quad (4b)$$

Where all input parameters retain their existing definitions as given in (2).

III. Measurements and Modelling

Rainfall drop size measurements undertaken using the Joss-Waldvogel (JW) disdrometer at these selected locations have been particularly useful in the estimation of the required input parameters for the DSD function in (2). Regarding the processing of the collected data, the first procedure is to obtain the DSD by means of computations provided in [12], given by:

$$N(D) = \frac{n_i}{ATv_t\Delta D_i} \quad [m^{-3}mm^{-1}] \quad (5)$$

Where n_i is the number of drops recorded by the measuring instrument, A is the sampling area of the measuring instrument giving by $0.005\ m^2$, v_t is the terminal velocity and ΔD_i is the diameter interval between successive classes of the 20 diameter channels.

The method of moment approach has been applied to obtain the input parameters of the Type II lognormal distribution in (2). To generate each nth moment, we employ the raw moment generating function given by [12], [13] and [15]:

$$M_n = N_T e^{\left[n\ln(D_g) + \frac{n^2 ln^2(\sigma_g)}{2}\right]} \quad (6)$$

For the drop size measurements, the moment for each recorded rain drop per channel can likewise be applied to generate the same moments as given in [15]:

$$M_n = \sum_{i=1}^{20} {D_i}^n N(D) \Delta D_i \quad (7)$$

Usually, the number of moments, n, required is exactly equal to the number of unknown parameters in the Type II lognormal distribution. These unknowns are estimated by equating (6) and (7) as the case may require. More information on this procedure can be found in [12], [13].

By following the procedure outlined in (5) – (7), unknown parameters in (2) at three African locations have been computed and 'refitted' as obtained from previous works in [15] and [16]. Table I presents a summary of the obtained parameters refitted for the Type II lognormal distribution obtained at Durban, Butare and Ile-Ife.

A cursory observation of these results reveal that there abound similarities in the functions obtained for σ_g and D_g across these locations, especially in the constants and quotients of rainfall rate. This may likely be due to the underlying and varying degree of tropical characteristics observed at these locations. Durban is a coastal South African location with subtropical climate; Butare is a Central African (Rwanda) location, equatorial in climate within intrinsic tropical weather; Ile-Ife is a Western African location with tropical climate. However, the functions obtained for N_T varies at all locations as this parameter is related to the spatial population of atmospheric rain drops during rain events. In Butare and Ile-Ife, where the tropical climate is more pronounced, the mechanism of droplet coagulation and aggregation often results in larger sizes of rain drops. However, in Durban, we find evidence of higher population of smaller rain drops during rainfall events [17]. While these are valid observations in the behaviour of these input parameters, it fails to fully explain their impacts on the actual profile of the DSD. This will be fully discussed in the section that follows.

TABLE I. PARAMETERS OF TYPE II LOGNORMAL DISTRIBUTION OBTAINED FOR DIFFERENT LOCATIONS IN AFRICA.

LOCATION	COORDINATES	PARAMETERS*		
		N_T	D_g	σ_g
Durban [15]	29°52′S, 30°58′E	$262.2R^{0.40}$	$0.73R^{0.15}$	$1.30R^{0.016}$
Butare [15]	2°36′S, 29°44′E	$95.6R^{0.304}$	$0.94R^{0.184}$	$1.31R^{0.40}$
Ile-Ife [16]	7°31′N, 4°31′E	$108R^{0.363}$	$0.82R^{0.199}$	$1.45R^{-0.021}$

*Functions therein have been approximated to significant values

IV. RESULTS AND DISCUSSION

The required parameters for the Type II lognormal distribution already obtained for different locations in Table I are applied as inputs to the proposed DEs in (3) and (4), by making D the independent variable. Results from (3) and (4) are usually found to be strongly dependent upon the intensity of rainfall events. Hence, the plots for these results are obtained for three possible categories of rainfall events: Showers (20 mm/h), thunderstorm (60 mm/h) and severe thunderstorm (110 mm/h). These categories are important thresholds that can help delineate the exact effects of differential impacts over different diametric spectrum.

Figure 1 presents the plots of the first and second derivatives of Type II lognormal distribution for the three locations at a rainfall rate of 20 mm/h (shower events). In each of these plots, we find that each of the derivative function for Durban measurements yields higher local maxima and local minima respectively. This is mainly the result of higher population of rain drops experienced at this location being a subtropical region. On the other hand, it is observed that the first and second derivative functions plotted for Butare and Ile-Ife are quite similar in shape. This is noticeable over all the entire range of diameters, implying that similar characteristics in DSD patterns can be found at these tropical and equatorial locations. An overview of the plots in 1(a) and 1(b) at 20 mm/h obtained also reveal that there is no significant contribution of rain drops for spherical droplet sizes beyond 2.5 mm, as the functions become 'flatlined'. This is mainly due to the absence of rain drops (from measurements) beyond this threshold.

Figure 2 presents first and second derivative plots at a rainfall rate of 60 mm/h - representing thunderstorm conditions. Again, the pattern observed here implies that the measurements at Durban remarkably have higher maxima and minima compared to measurements at Butare and Ile-Ife. In addition, the differential DSD characteristics at Butare and Ile-Ife still behave similar in shape, complementing the strong tropical characteristics at these locations. An overview of the plots obtained in 2(a) and 2(b) indicate that the contributions of rain drops to attenuation is not remarkable for spherical droplets sizes beyond 3.5 mm. Flatlining of the derivative functions also becomes observable beyond this threshold due to the earlier explained reason.

In Figure 3, the first and second derivative plots at 110 mm/h (severe thunderstorm) are not entirely different from the pattern previously observed at Figure 1 and Figure 2. Although, there is a little deviation in the local minima and local maxima of the functions obtained at Butare and Ile-Ife, these functions are actually the same, except for amplitudinal differences. Also, the peaks observed in the measurements at Durban far exceeds those observed at the two other locations. Also, an overview of the plot shows that no significant contributions to rain attenuation will be added by rain drops of spherical droplet sizes beyond 4 mm.

V. CONCLUSION

This study has approached the subject of understanding the variation of DSD over different diameters at selected locations in Africa. This is important in investigating the rain drop measurements at different parts of the world. Based on the results obtained, it becomes easier to see that the application of derivatives to a typical DSD function can assist in

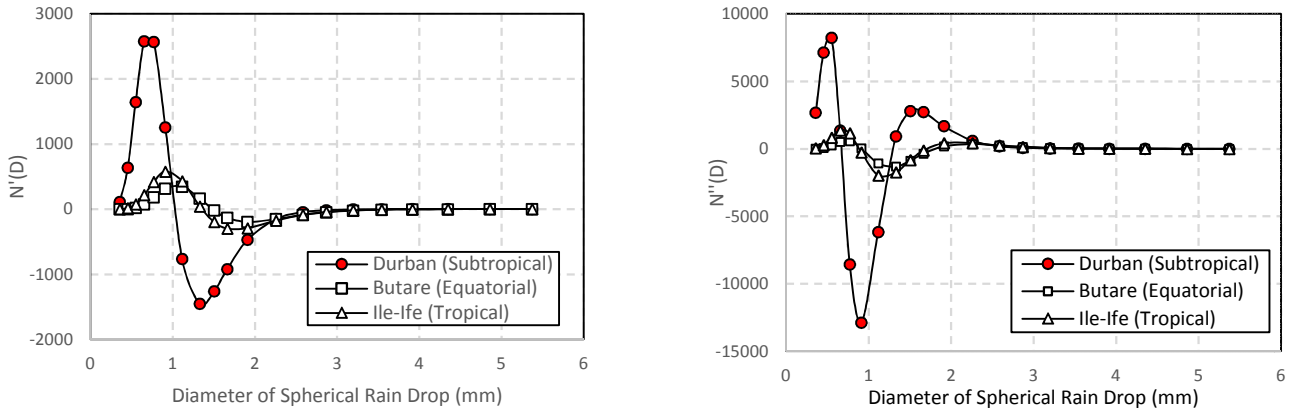

(*a*) (*b*)

Fig. 1. Plots of lognormally-distributed differential functions versus spherical rain drop diameters at different locations at a rain rate of 20 mm/h (*a*) First derivative (*b*) Second derivative.

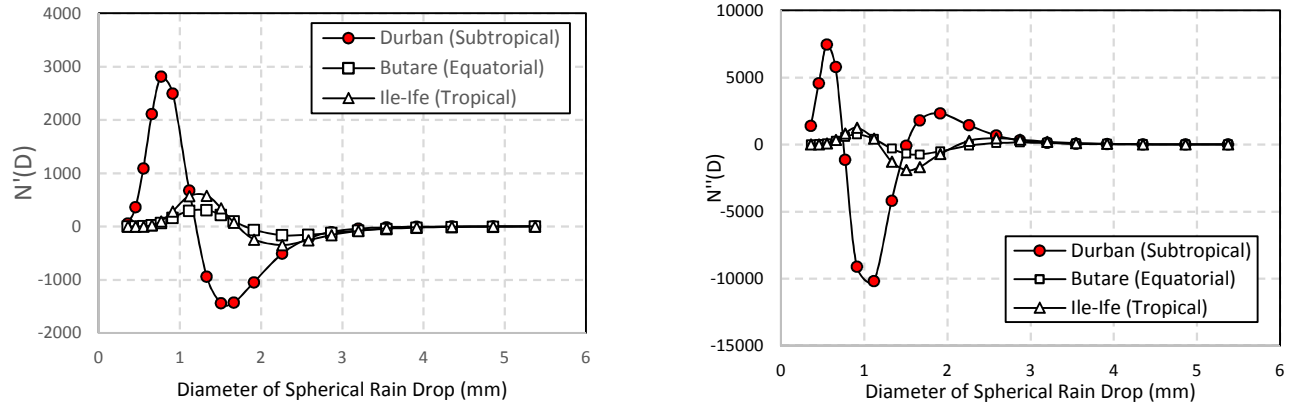

(*a*) (*b*)

Fig. 2. Plots of lognormally-distributed differential functions versus spherical rain drop diameters at different locations at a rain rate of 60 mm/h (*a*) First derivative (*b*) Second derivative.

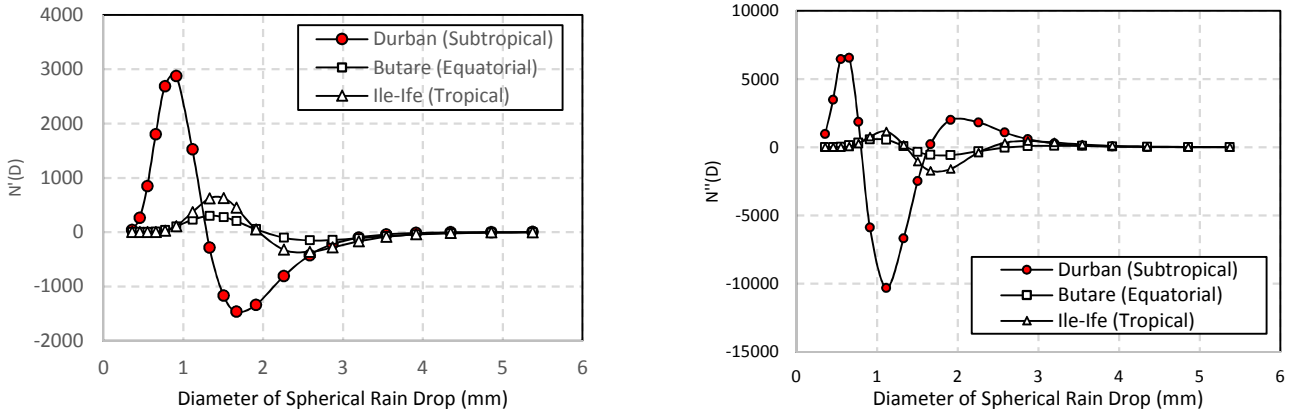

(*a*) (*b*)

Fig. 3. Plots of lognormally-distributed differential functions versus spherical rain drop diameters at different locations at a rain rate of 110 mm/h (*a*) First derivative (*b*) Second derivative.

understanding the active population of atmospheric rain drops. Since these population contribute to scattering and absorption of transmission signals during local rain event, this tool can be employed in the informed analysis of DSDs at different locations around the world. It is important to note that this tool is still being studied (and further developed) to understand its extensive usefulness in rainfall attenuation for 5G communication. It is hoped that more promising results will be presented in the nearest future concerning the subject of rain drop sizes, and its impact on wireless communication.

REFERENCES

[1] D. Wang, D. Chen, B. Song, N. Guizani, X. Yu and X. Du, "From IoT to 5G I-IoT: The Next Generation IoT-Based Intelligent Algorithms

and 5G Technologies," in *IEEE Communications Magazine*, vol. 56, no. 10, pp. 114-120, Oct. 2018.

[2] D. Foty, B. Smith, S. Sinha and M. Schröter, "The wireless bandwidth crisis and the need for power-efficient bandwidth," *ISSCS 2011 - International Symposium on Signals, Circuits and Systems*, Lasi, 2011, pp. 1-6

[3] D. Foty, B. Smith, S. Sinha and M. Schröter, "Expanding wireless bandwidth in a power-efficient way: developing a viable mm-wave radio technology," *East-West Design & Test Symposium (EWDTS 2013)*, Rostov-on-Don, 2013, pp. 1-6.

[4] A. I. Sulyman, A. Alwarafy, G. R. MacCartney, T. S. Rappaport and A. Alsanie, "Directional Radio Propagation Path Loss Models for Millimeter-Wave Wireless Networks in the 28-, 60-, and 73-GHz Bands," in *IEEE Transactions on Wireless Communications*, vol. 15, no. 10, pp. 6939-6947, Oct. 2016

[5] "5G Spectrum: GSMA Public Policy Position", GSM Association,. Nov. 2018.

[6] A. Alonge and T. Afullo, "60GHz millimeter-wave radio in South Africa: Link design feasibility and prospects," *2016 Progress in Electromagnetic Research Symposium (PIERS)*, Shanghai, 2016, pp. 3686-3691.

[7] M. U. Sheikh, J. Säe and J. Lempiäinen, "Multipath Propagation Analysis of 5G Systems at Higher Frequencies in Courtyard (Small Cell) Environment," *2018 IEEE 5G World Forum (5GWF)*, Silicon Valley, CA, 2018, pp. 239-243..

[8] M. Khalily, M. Ghoraishi, S. Taheri, S. Payami and R. Tafazolli, "Millimeter-wave directional path loss models in the 26 GHz, 32 GHz, and 39 GHz bands for small cell 5G cellular system," *12th European Conference on Antennas and Propagation (EuCAP 2018)*, London, 2018, pp. 1-5

[9] R. Crane, "Prediction of Attenuation by Rain," in *IEEE Transactions on Communications*, vol. 28, no. 9, pp. 1717-1733, September 1980.

[10] "Characteristics of Precipitation for Propagation Modelling," ITU-R, Geneva, 2017, ITU-R Rec. P.837-7.

[11] M. O. Odedina and T. J. Afullo, "Determination of rain attenuation from electromagnetic scattering by spherical raindrops: Theory and experiment," in *Radio Science*, vol. 45, no. 01, pp. 1-15, Feb. 2010.

[12] A.A. Alonge and T.J.O. Afullo, "Seasonal Analysis and Prediction of Rainfall Effects in Eastern Southern Africa at Microwave Frequencies," *Progress in Electromagnetic Research B*, vol. 40, pp. 279-303, 2012.

[13] K. I. Timothy, Jin Teong Ong and E. B. L. Choo, "Raindrop size distribution using method of moments for terrestrial and satellite communication applications in Singapore," in *IEEE Transactions on Antennas and Propagation*, vol. 50, no. 10, pp. 1420-1424, Oct. 2002.

[14] G. Feingold and Z. Levin, "The lognormal Fit to Raindrop Spectra from Frontal Convective Clouds in Israel," Journal of Climate and Applied Meteorology, Vol. 25(10), pp. 1346-1363, Oct. 1986

[15] A. A. Alonge and T. J. Afullo, "Rainfall microstructures for microwave and millimeter wave link budget at tropical and subtropical sites," *2013 Africon*, Pointe-Aux-Piments, 2013, pp. 1-5.

[16] G.O. Ajayi. and R. L. Olsen, "Modeling of a tropical raindrop size distribution for microwave and millimetre wave applications," *Radio Sci.*, Vol. 20, No. 2, 193-202, April 1985.

[17] A. A. Alonge and T. J.Afullo, "Rainfall Microstructural Analysis for Microwave Link Networks: Comparison at Equatorial and Subtropical Africa," *Progress in Electromagnetic Research B*, vol. 59, pp. 45-58, 2014.